Energy, Environment and Storage

Journal Homepage: www.enenstrg.com

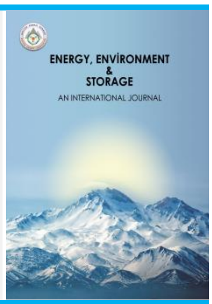

Theoretical Study of The Use of Lfscs in Terms of Energy for Textile Factories: The Example of Saint Louis in Senegal

Issa SY[1*], İbrahim ÜÇGÜL[2]

[1]*Graduate School of Natural and Applied Sciences, Department of Renewable Energy, Süleyman Demirel University, Isparta, Turkey, ORCID: 0000-0001-9889-4783.*
[2]*Department of Textile Engineering, Faculty of Engineering, Süleyman Demirel University, Isparta, Turkey, 0000-0001-9794-0653.*

ABSTRACT. Senegal has a high potential for solar energy but mainly depends on fossil energy resources. Industries, particularly the textile sector, could benefit from the use of alternative energy sources to reduce costs and improve the environmental footprint. This study focuses on the use of linear Fresnel solar collectors (LFSC) coupled with an Organic Rankine Cycle (ORC) system to produce energy in textile mills, particularly in Saint Louis. The objective was to size a Fresnel solar array and evaluate its energy production for two different periods: the sunniest month (April) and the least sunny month (August). The findings demonstrate the substantial solar potential of the region, with significant sunshine throughout the year. The maximum direct solar radiation recorded on August 15 and April 25 was 898 W/m2 and 945 W/m2, respectively, at noon. The maximum energy production for one row in August is 24.4 kWh, and in April, it reaches 25.7 kWh. It is noted that, for the use of the Fresnel linear system, the number of rows will depend on the energy needs of the textile factory.

Keywords: *Solar energy, Linear Fresnel Reflector, concentrating solar power, Senegal.*

Article History: Received: 15.03.2023; Accepted:19.03.2023; Available Online: 29.05.2023
Doi: https://doi.org/10.52924/PIBX6890

1. INTRODUCTION

Located in the extreme west of Africa between 12°5 and 16°5 North latitude and 11°5 and 17°5 West longitude, Senegal covers an area of 196.712 km2. Like many countries in Africa, solar energy is abundant in Senegal. The whole country is sunny and receives a level of global horizontal sunshine between 2045 and 2191 kWh/m2 /year and 1461 of 1607 kWh/m2 /year of direct radiation. That is 3,000 hours of sunshine per year and an average daily solar irradiation of 5.8 kWh/m2/day [1]. The solar potential maps show that the global horizontal irradiation (GHI) in the centre and north averages about 2170 kWh/m²/year. For direct normal irradiation (DNI), the annual average is about 1607 in a large part of the north, like Saint Louis. The energy sector is essentially dependent on the outside world due to the predominance of fossil energy resources (petroleum products and other hydrocarbons) which the country does not possess. Although the country has many natural resources whose energy potential is proven very little exploited.

Senegal's exports have grown stronger thanks to the development of manufacturing industries. After independence, industries diversified and improved the quality of their products to meet the growing demand of the domestic market and neighbouring countries. In the textile sector, the use of solar energy can be a promising solution to reduce operating costs and improve the environmental footprint of the industry.

Production costs have increased considerably with the rise in energy prices, and this can affect the competitiveness of companies. Thus, the use of alternative energy sources is becoming an important option for these industries [2]. In this respect and with the current context of climate change, there is a need to think about the use of more sustainable resources[3]. Renewable energy resources are seen as one of the most efficient solutions [4]. Alrikabi et al (2014) [5] worked on the types of renewable energy sources. Their results show that by promoting renewable energy, air pollution, soil pollution and water pollution can be avoided and a country's economy will increase. The use of renewable energies and particularly solar thermal energy is one of the most promising strategies [6]. The production of thermal energy is based on concentrating solar power technologies. These technologies use collectors to concentrate solar radiation onto absorbers, which heat a heat transfer fluid to a high temperature. This fluid can then be used to generate electricity [7]. Two types of solar concentrators can be distinguished: point concentrators, which track the sun on two axes, such as tower plants and Stirling Dish plants, and linear concentrators, which track the sun on one axis, such as parabolic trough concentrators and Fresnel mirrors [8]. These systems offer several advantages, such as their ability to concentrate sunlight and their suitability for industrial applications [9]. Industries, known for their substantial energy consumption, can particularly benefit from the integration of LFSCs to reduce their reliance on fossil fuels [10].

This study focuses on investigating the potential of LFSCs for energy production in textile factories, using the case of Saint Louis in Senegal as an example. By examining the technical aspects of LFSC implementation in this specific context, this study aims to provide valuable insights for similar settings globally. The primary objective of this research is to assess the energy output of LFSCs in textile factories, employing an Organic Rankine Cycle (ORC) system as a conversion mechanism. By analyzing the results at different times of the year, this study aims to determine the system's performance under varying solar conditions. To achieve these objectives, a theoretical approach is adopted, encompassing the sizing of the Fresnel solar array and the evaluation of energy production.

Overall, this theoretical study serves as a foundation for assessing the feasibility and potential benefits of integrating LFSCs in textile factories, taking into account the specific case of Saint Louis in Senegal. The findings will not only contribute to the existing knowledge on solar energy utilization but also provide valuable insights for industries seeking sustainable energy solutions. This work will be one of the first steps in the use of Linear Fresnel Solar Collectors in the area.

2. SOLAR ENERGY

2.1 Solar radiation

Solar energy is an energy source that comes from the sun's rays. It is considered to be the most powerful source of energy and is also free and easy to use. The calculation of the total incident solar radiation on an exposed surface depends on several factors, such as the geographical position of the surface, the time of day, the season, the orientation and inclination of the surface, and the weather conditions. Direct radiation is given by:

$$\mathrm{I_d} = \mathrm{I_{DN}} \times \cos(\theta_s) \tag{1}$$

With θ_s the value of the angle of incidence of the sun.
And

$$\mathrm{I_{DN}} = \mathrm{A_1} \times \exp\left(-\frac{\mathrm{P_L}}{\mathrm{P_o}} \times \frac{\mathrm{B}}{\sin(\mathrm{h})}\right) \tag{2}$$

Where:

$\frac{P_L}{P_o}$ is the pressure ratio at the location concerned with the standard atmospheric pressure.

A_1 is the extraterrestrial solar intensity.

B is the atmospheric absorption coefficient.

h is the angular height

$$\frac{\mathrm{P_L}}{\mathrm{P_o}} = \exp(-0.0001184 \times \mathrm{H_{alt}}) \tag{3}$$

$$\mathrm{A_1} = 1158 \times \left[1 + 0.066 \times \cos\left(360 \times \frac{\mathrm{n}}{370}\right)\right] \tag{4}$$

$$\mathrm{B} = 0.175 \times [1 - 0.2 \times \cos(0.93 \times \mathrm{n})] - 0.0045 \times [-\cos(1.86 \times \mathrm{n})] \tag{5}$$

H_{alt} is the altitude in metres above sea level.

n is the number of days in the year between 1 and 365 or 366 (leap year).

2.2 Solar energy technologies

Technologies for the exploitation of solar energy are divided into two categories: active and passive technologies. Active technologies convert solar energy directly into electrical or thermal energy, such as photovoltaic cells, solar collectors, solar concentrators, solar heating and cooling systems, and solar cookers. Passive technologies, on the other hand, focus on the orientation of buildings to the sun and the use of special materials and architectural designs to harness solar energy [11].

Solar concentrators usually consist of two components: the concentrator and the receiver. The concentrator reflects the sun's rays to the receiver. The receiver acts as a heat exchanger that converts the solar flux reflected by the mirrors into heat. This heat is then used to produce electrical energy or for cogeneration. There are four main technologies of concentrating solar power plants for electricity generation: the tower plant, the parabolic trough plant, the parabolic or Dish plant and the linear Fresnel plant [12].

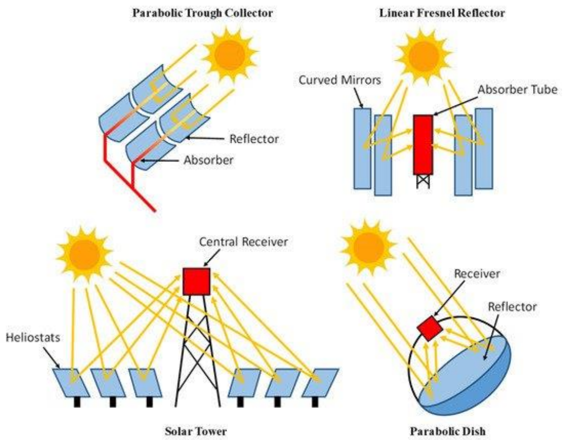

Fig. 1. Different types of solar concentrators [13]

Fresnel technology uses flat mirrors arranged to form a parabolic cylinder shape. These mirrors are equipped with a motorised system that allows them to follow the sun on a single axis, to concentrate the rays towards a linear receiver located on the focal length. This solar power plant uses a working fluid, which can be oil or water [14].

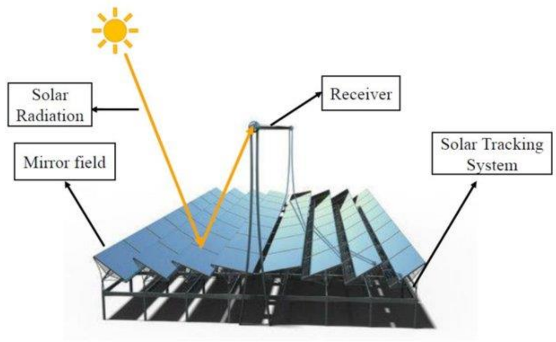

Fig. 2. Linear Fresnel Reflector system representation *[15]*

Linear Fresnel collectors have been used because they have the advantage of being cheaper to produce and install. They also require less reflective material and are easier to maintain. In addition, linear Fresnel collectors can be more flexible in terms of size and shape, which can be an advantage for projects where space is limited. They can also be adapted to operate with different working fluids, such as oil or water, allowing them to meet a variety of energy needs.

3. METHODOLOGY

3.1 Model sizing

The Fresnel concentrator principle is based on mirrors that can be rotated to follow the path of the sun to permanently redirect and concentrate the sun's rays to a fixed linear receiver tube or set of tubes. By circulating through this horizontal receiver, a thermodynamic liquid of up to 550°C can be vaporised and superheated. The steam produced then drives a turbine which generates electricity [16].

According to [17] linear Fresnel solar collectors can be designed using two different methods. In the first method, a fixed receiver width and height are chosen, from which variable mirror dimensions, mirror angles and inter-mirror distances can be calculated. In the second method, the one used in this work, the mirror widths and receiver height are fixed and the other device parameters are determined by simple equations.

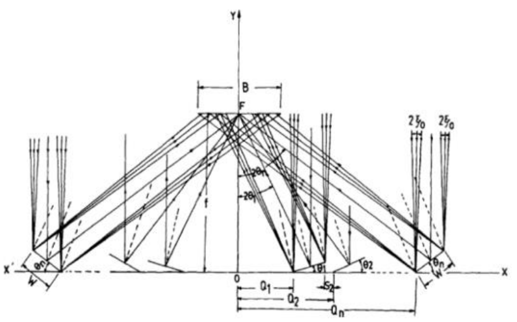

Fig. 3. Schematic modelling of an LFRSC *[17]*

In this model, each mirror is characterised by three parameters:

- ✓ the angle of the mirrors θ_n ;
- ✓ the distance between the mirror and the receiver Q_n ;
- ✓ the offset between two adjacent mirrors S_n.

$$\theta_n = \frac{1}{2}\tan^{-1}\left[\frac{Q_n + \frac{W}{2}\cos(\theta_{n-1})}{f + \frac{W}{2}\sin(\theta_{n-1})}\right] \quad (6)$$

$$Q_n = Q_{n-1} + W \times \cos(\theta_{n-1}) + S_n \quad (7)$$

$$S_n = W \times \sin(\theta_{n-1}) \times \tan(2\theta_n + \xi_0) \quad (8)$$

In these equations:

W is the width of the mirrors, f the height of the absorber above the plane mirrors and the index n is the mirror number.

ξ_0 is half the apparent angle of the sun at any point on the Earth. The initial values of the various design parameters are given [17] :

$\theta_0 = 0$, $\xi_0 = 16°$, $S_1 = 0$, $Q_1 = \frac{W}{2}$ et $Q_0 = -\frac{W}{2}$.

The receiver width design can be calculated based on the data calculated for the last mirror using the formula below.

$$B = 2\left[\left(Q_k + \frac{W}{2}\cos\theta_k \sec 2\theta_k\right)\frac{\sin\xi_0}{\sin 2\theta_k \cos(2\theta_k + \xi_0)} + \frac{W}{2}\cos\theta_k \sec 2\theta_k\right] \quad (9)$$

Here k represents the number of mirrors in a dimension.

The concentration ratio (CR) of the Fresnel collector can be determined by adding the concentration contribution of the mirrors (CIn).

$$CR = 2\sum_{n=1}^{n=k} CI_n \quad (10)$$

$$CIn = \frac{W \times \cos\theta_n}{U_n + D_n + I_n} \quad (11)$$

With U_n, D_n and the values of the reflected solar rays.

$$U_n = \left(\frac{Q_n + W\cos\theta_n - \frac{W}{2}\cos\theta_n \sec 2\theta_n}{\sin 2\theta_n}\right)\frac{\sin\xi_0}{\cos(2\theta_n - \xi_0)} \quad (12)$$

$$D_n = W \times \cos\theta_n \sec 2\theta_n \quad (13)$$

$$I_n = \left(\frac{Q_n + \frac{W}{2}\cos\theta_n \sec 2\theta_n}{\sin 2\theta_n}\right)\frac{\sin\xi_0}{\cos(2\theta_n - \xi_0)} \quad (14)$$

3.2 Energy balance and efficiency

The useful thermal power of the solar array is calculated by subtracting the thermal losses from the total absorbed power [18].

$$Q_{field} = Q_{inc} - Q_{loss} \quad (15)$$

The thermal power absorbed by the absorber tube and the thermal losses of the Fresnel field are calculated according to [18].

$$Q_{inc} = \eta_{opt,0} \times K_t \times K_l \times \eta_{endloss} \times cl \times \chi_{field} \times A_{ST} \times I_d \quad (16)$$

$$Q_{loss} = A_{field} \times 0.0724\frac{W}{m^2} \times (-0.389 \times \Delta T + 0.0108 \times \Delta T^2) + A_{ST} \times q_{pipeloss} \quad (17)$$

In these equations, $\eta_{opt,0}$ is the efficiency of the optical collector for the perpendicular sun on collector, cl being the average cleaning factor, χ_{field} being the solar field availability, A_{ST} is the total collector opening area and ΔT is the temperature difference between the average temperature of the fluid in the solar field and the ambient temperature.

$$\Delta T = \frac{T_{in}+T_{out}}{2} - T_{amb} \tag{18}$$

$\eta_{endloss}$ is the final loss efficiency, it describes the amount of the receiver that is not illuminated by the reflected rays [19].

$$\eta_{endloss} = 1 - \frac{f \times \tan(\theta_l)}{Lm} \tag{19}$$

$K_t(\theta_t)$ is the correction factor for the angle of incidence in the transverse plane;

$K_l(\theta_l)$ is the correction factor for the angle of incidence in the longitudinal plane[20].

$$K_l(\theta_l) = \cos(\theta_l) - \frac{f}{L_m}\sqrt{1+\left(\frac{W_D}{4f}\right)^2} \times \sin(\theta_l) \tag{20}$$

$$K_t(\theta_t) = \begin{cases} \cos\left(\frac{\theta_t}{2}\right) - \frac{\frac{W_D}{4}}{f+\sqrt{f^2+\left(\frac{W_D}{4f}\right)^2}} \times \sin\left(\frac{\theta_t}{2}\right), & \text{when the } \theta_t < \theta_{t,crit} \\ \left[\cos\left(\frac{\theta_t}{2}\right) - \frac{\frac{W_D}{4}}{f+\sqrt{f^2+\left(\frac{W_D}{4f}\right)^2}} \times \sin\left(\frac{\theta_t}{2}\right)\right] \times \left[\frac{D_W}{W} \times \frac{\cos(\theta_t)}{\cos\left(\frac{\theta_t+\varphi m}{2}\right)}\right], & \text{when the } \theta_t \geq \theta_{t,crit} \end{cases} \tag{21}$$

Where:

$$\varphi_m = 2\arctan \frac{\frac{W_D}{4}}{\left[f+\sqrt{f^2+\left(\frac{W_D}{4f}\right)^2}\right]} \tag{22}$$

And:

$$\theta_{t,crit} = 94.46 - 2.519\frac{W}{D_W} - 55.71\left(\frac{W}{D_W}\right)^2 - 0.48\varphi_m + 1.77\frac{{\varphi_m}^2}{1000} + 1.15\frac{W}{D_W}\varphi_m \tag{23}$$

Equations (19) and (20) are valid only for $20° < \varphi_m < 70°$ and $0.50 < (\frac{W}{D_W}) < 0.95$ [21].

4. RESULTS AND DISCUSSIONS

4.1 The parameters of the Fresnel system model

The MATLAB program was used to calculate the mirrors and their distances and the results are given in Table 1. In the calculations, the width of the mirrors W was fixed at 0.40 m, the length at 40 m and the height of the absorber above the plane mirrors f to 6 m.

Table 1 Result of the mirror data of the linear Fresnel collector.

	M 1	M 2	M3	M 4	M 5	M 6	M7
Q	0.20	0.60161	1.00618	1.41555	1.82998	2.25131	2.68086
θ	1.907	3.8002	6.1181	7.5044	9.3011	11.0468	12.7385

It is important to note that these results were obtained for one side of the receiver. Being symmetrical, the same data is used for the other side. After calculating all the necessary parameters for the mirror, the width of the receiver found according to the data calculated for the last mirror is 0.502 m.

The concentration ratio (CR) of the Fresnel collector can be determined by adding the concentration contribution of the mirrors (CIn). The results are given in Table 2.

Table 2 Result of Condensation Rate Coefficients and Condensation Rate vs. Mirrors.

	A	Dn	In	Cln
Mirror 1	2.8003	40.0666	2.8065	0.8753
Mirror 2	2.8362	40.2658	2.8488	0.8686
Mirror 3	2 .6947	40.6967	2.7154	0.8626
Mirror 4	2.9861	41.0580	3.0121	0.8428
Mirror 5	3.0994	41.6501	3.1329	0.8244
Mirror 6	3.2419	42.3700	3.2833	0.8029
Mirror 7	3.4142	43.2181	3.4645	0.7788
Total on one side				**5.8554**
Concentration ratio				**11.71075**

4.2 Solar Irradiation and thermal energy

According to the meteorology of the site, the energy production was calculated in August with the lowest direct solar radiation and in April with good radiation [22]. The amount of direct solar radiation (Id) and the instantaneous thermal energy (Qfield) that can be provided by the solar field was obtained from 07:00 to 17:00 on August 15 and April 25.

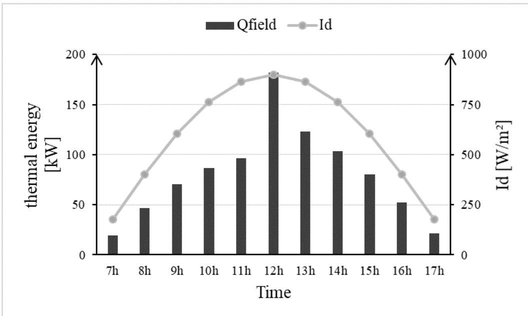

(a) August

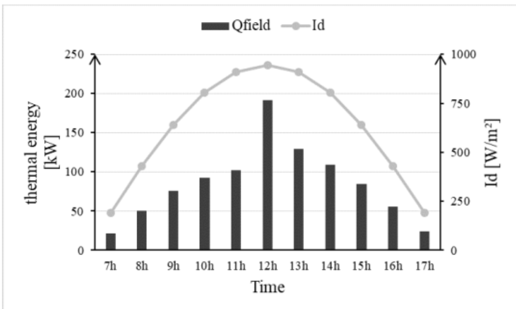

(b) April

Fig. 4. Direct solar radiation and instantaneous thermal energy on August 15 (a) and April 25 (b).

Fig. 4 shows the amount of direct solar radiation and the instantaneous thermal energy that the solar field can provide, measured from 7:00 am to 5:00 pm on August 15

(a) and April 25 (b). The results show that the region has a large solar potential and that all months have significant sunshine.

4.3 Energy production with the organic Rankine cycle (ORC)

The organic Rankine cycle is a thermodynamic process used to convert heat into electrical energy using the system's output temperature. The choice of organic fluid used in the ORC system is critical for its efficiency and performance. For this process, R152a was chosen as the organic fluid. According to [23], it gives a good working efficiency of the turbine and a high cycle efficiency. The energy production calculations were carried out using the Solkane 8 software. The input parameters are as follows: T_{Evap} = 100 °C, T_{cond} = 40 °C, Turbine-efficiency = 0.98 and Pump- efficiency = 0.89. To evaluate the electrical energy produced by the ORC turbine system, the amounts of useful heat transferred to the heat transfer fluid between 7 a.m. and m. were taken in Table 3. These data were collected for one row on August 15 and April 25.

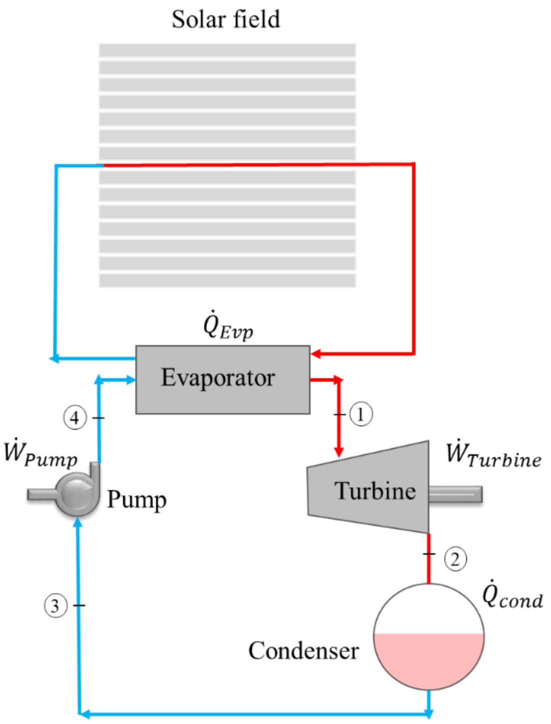

Fig. 5. ORC system representation.

Table 3 The values of energy production obtained by a row of the organic Rankine system.

Time	$\dot{Q}_{Evp}$ (kWh)	$\dot{Q}_{cond}$ (kWh)	$\dot{W}_{Turbine}$ (kWh)	$\dot{W}_{Pump}$ (kWh)	$\dot{W}_{net}$ (kWh)	η_{th}
7h	19.45	17.04	2.66	0.28	2.6	0.12
8h	46.87	41.07	6.4	0.68	6.28	0.12
9h	70.62	61.89	9.65	1.03	9.46	0.12
10h	86.66	75.9	11.8	1.3	11.6	0.12
11h	96.56	84.6	13.2	1.4	12.9	0.12
12h	181.87	159.4	24.9	2.6	24.4	0.12
13h	123.13	107.9	16.8	1.8	16.5	0.12
14h	103.39	90.6	14.1	1.5	13.8	0.12
15h	79.96	70.1	10.9	1.2	10.7	0.12
16h	51.97	45.54	7.1	0.76	6.96	0.12
17h	21.47	18.81	2.93	0.31	2.88	0.12

(a) August

Time	$\dot{Q}_{Evp}$ (kWh)	$\dot{Q}_{cond}$ (kWh)	$\dot{W}_{Turbine}$ (kWh)	$\dot{W}_{Pump}$ (kWh)	$\dot{W}_{net}$ (kWh)	η_{th}
7h	21.61	18.94	2.95	0.31	2.89	0.12
8h	50.51	44.26	6.9	0.74	6.76	0.12
9h	75.47	66.1	10.3	1.1	10.1	0.12
10h	92.30	80.9	12.6	1.3	12.4	0.12
11h	101.87	89.3	13.9	1.5	13.6	0.12
12h	191.56	167.9	26.2	2.8	25.7	0.12
13h	129.15	113.2	17.6	1.9	17.3	0.12
14h	108.83	95.4	14.9	1.6	14.6	0.12
15h	84.74	74.3	11.6	1.2	11.3	0.12
16h	55.59	48.71	7.6	0.81	7.44	0.12
17h	23.69	20.76	3.24	0.35	3.17	0.12

(b) April

The table above shows the values of energy production obtained by a row of the organic Rankine system on 15 August (a) and 25 April (b). In this context, the expressions $\mathbf{\dot{Q}_{Evp}}$ represent the amount of energy entering the evaporator (kWh), $\dot{Q}_{cond}$ the amount of energy drawn from the condenser (kWh), $\dot{W}_{Turbine}$ the amount of energy obtained in the turbine (kWh), $\dot{W}_{Pump}$ the amount of energy needed to operate the pump (kWh), and finally $\dot{W}_{net}$ corresponds to the net electricity produced by the system (kWh). The cycle efficiency is defined as the ratio between the net powers of the cycle to the evaporator heat rate. The results show that the maximum amount of energy obtained in August is 24.4 kWh, while in April it reaches 25.7 kWh. Despite a slightly small difference, both values indicate a high solar potential in the region. Indeed, all months of the year are almost equally sunny, with a slight variation. These results have implications for the size of a linear Fresnel system, which will depend on the energy needs of the textile factory. For example, to produce 500 kWh, 20 collector rows would be required.

5. CONCLUSION

The use of linear Fresnel solar collectors in textile mills can have many economic and environmental benefits. This work focused on the use of linear Fresnel solar collectors (LFSC) for energy production in textile factories, using the example of Saint Louis, Senegal. After sizing the Fresnel solar array, the energy output was assessed using the ORC at two distinct times: the month with the most sunshine (April) and the month with the least sunshine (August). The organic fluid R152a and the Solkane program were used to calculate the electricity production.

The results show that the region has a large solar potential and that all months have significant sunshine. According to the calculations, the maximum direct solar radiation obtained on August 15 and April 25 was 898 W/m^2 and 945 W/m^2, respectively. These values were produced at 12:00 pm. With a single collector row, energy production amounts to 24.4 kWh during the month of August, while in April it reaches 25.7 kWh. In addition, the thermal efficiency of the system is 12%. To optimise the needs of a textile factory it is necessary to multiply the number of rows. The use of this technology is a viable solution for companies seeking to reduce their dependence on fossil fuels and improve their environmental impact. Therefore, it is important that companies study the economic cost of implementing such a system of linear Fresnel solar collectors for energy production.

REFERENCES

[1] N. Diaw and T. T. Soe, ‘Estimation of Solar Potential in Senegal Using GIS Application’, *International Journal of Advanced Research*, vol. 4, no. 1, p. 5, 2017.

[2] B. Tchanche, ‘Analyse du système énergétique du Sénégal’, *Revue des Energies Renouvelables*, vol. 21, no. 1, pp. 73–88, 2018.

[3] Y. Mochizuki and A. Bryan, ‘Climate Change Education in the Context of Education for Sustainable Development: Rationale and Principles’, *Journal of Education for Sustainable Development*, vol. 9, no. 1, pp. 4–26, Mar. 2015, doi: 10.1177/0973408215569109.

[4] I. Dincer, ‘Renewable energy and sustainable development: a crucial review’, *Renewable and Sustainable Energy Reviews*, vol. 4, no. 2, pp. 157–175, Jun. 2000, doi: 10.1016/S1364-0321(99)00011-8.

[5] N. Kh. M. A. Alrikabi, ‘Renewable Energy Types’, *JOCET*, vol. 2, no. 1, pp. 61–64, 2014, doi: 10.7763/JOCET.2014.V2.92.

[6] D. Qerimi, C. Dimitrieska, S. Vasilevska, and A. A. Rrecaj, ‘Modeling of the Solar Thermal Energy Use in Urban Areas’, *Civ Eng J*, vol. 6, no. 7, pp. 1349–1367, Jul. 2020, doi: 10.28991/cej-2020-03091553.

[7] V. Siva Reddy, S. C. Kaushik, K. R. Ranjan, and S. K. Tyagi, ‘State-of-the-art of solar thermal power plants—A review’, *Renewable and Sustainable Energy Reviews*, vol. 27, pp. 258–273, Nov. 2013, doi: 10.1016/j.rser.2013.06.037.

[8] M. Saini, A. Sharma, V. P. Singh, G. Dwivedi, and S. Jain, ‘Solar Thermal Receivers—A Review’, in *Advancement in Materials, Manufacturing and Energy Engineering, Vol. II*, P. Verma, O. D. Samuel, T. N. Verma, and G. Dwivedi, Eds., in Lecture Notes in Mechanical Engineering. Singapore: Springer Nature, 2022, pp. 311–325. doi: 10.1007/978-981-16-8341-1_25.

[9] K. B. Kumar, M. Gupta, and D. S. Mehta, ‘Efficient sunlight harvesting with combined system of large Fresnel lens segmented mirror reflectors and compound parabolic concentrator without tracking sun for indoor daylight illumination’, *Renewable Energy*, vol. 202, pp. 1198–1214, Jan. 2023, doi: 10.1016/j.renene.2022.11.117.

[10] F. J. Sepúlveda *et al.*, ‘Analysis of Potential Use of Linear Fresnel Collector for Direct Steam Generation in Industries of the Southwest of Europe’, *Energies*, vol. 12, no. 21, p. 4049, Oct. 2019, doi: 10.3390/en12214049.

[11] C. Firat and K. Çalik, ‘Electrical and Thermal Performance Analysis of a Linear Fresnel Reflector-Photovoltaic/Thermal System’, *Academic Platform Journal of Engineering and Science*, vol. 9, no. 2, pp. 264–273, May 2021, doi: 10.21541/apjes.778563.

[12] A.-G. Jolivot, ‘Conception et dimensionnement d’un récepteur linéaire pour un concentrateur de type Fresnel’, 2015.

[13] M. Toub, C. R. Reddy, R. D. Robinett, and M. Shahbakhti, ‘Integration and Optimal Control of MicroCSP with Building HVAC Systems: Review and Future Directions’, *Energies*, vol. 14, no. 3, p. 730, Jan. 2021, doi: 10.3390/en14030730.

[14] M. J. Montes, C. Rubbia, R. Abbas, and J. M. Martínez-Val, ‘A comparative analysis of configurations of linear Fresnel collectors for concentrating solar power’, *Energy*, vol. 73, pp. 192–203, Aug. 2014, doi: 10.1016/j.energy.2014.06.010.

[15] P. Scalco, J. Copetti, M. H. Macagnan, and J. Diehl de Oliveira, ‘Linear Fresnel Solar Collector Concentrator - A Review’, in *Proceedings of the 26th International Congress of Mechanical Engineering*, ABCM, 2021. doi: 10.26678/ABCM.COBEM2021.COB2021-0132.

[16] M. Ghodbane, B. Boumeddane, Z. Said, and E. Bellos, ‘A numerical simulation of a linear Fresnel solar reflector directed to produce steam for the power plant’, *Journal of Cleaner Production*, vol. 231, pp. 494–508, Sep. 2019, doi: 10.1016/j.jclepro.2019.05.201.

[17] S. S. Mathur, T. C. Kandpal, and B. S. Negi, ‘Optical design and concentration characteristics of linear Fresnel reflector solar concentrators—II. Mirror elements of equal width’, *Energy Conversion and Management*, vol. 31, no. 3, pp. 221–232, Jan. 1991, doi: 10.1016/0196-8904(91)90076-U.

[18] G. Morin, J. Dersch, W. Platzer, M. Eck, and A. Häberle, ‘Comparison of Linear Fresnel and Parabolic Trough Collector power plants’, *Solar Energy*, vol. 86, no. 1, pp. 1–12, Jan. 2012, doi: 10.1016/j.solener.2011.06.020.

[19] Y. Elmaanaoui and D. Saifaoui, ‘Parametric analysis of end loss efficiency in linear Fresnel reflector’, in *2014 International Renewable and Sustainable Energy Conference (IRSEC)*, Ouarzazate, Morocco: IEEE, Oct. 2014, pp. 104–107. doi: 10.1109/IRSEC.2014.7059813.

[20] E. Bellos, ‘Progress in the design and the applications of linear Fresnel reflectors – A critical review’, *Thermal Science and Engineering Progress*, vol.

10, pp. 112–137, May 2019, doi: 10.1016/j.tsep.2019.01.014.

[21] M. Ghodbane, Z. Said, A. A. Hachicha, and B. Boumeddane, 'Performance assessment of linear Fresnel solar reflector using MWCNTs/DW nanofluids', *Renewable Energy*, vol. 151, pp. 43–56, May 2020, doi: 10.1016/j.renene.2019.10.137.

[22] 'Saint-Louis : Climat, Températures et Météo. Les meilleures périodes !(SENEGAL)', *www.partir.com*. https://www.partir.com/Senegal/Saint-Louis/2246452/quand-partir.html (accessed Mar. 13, 2023).

[23] P. Prabowo., A. G.T., and E. Ekadewi., 'Performance of Organic Rankine Cycle in Different Refrigerants for Low Temperature Geothermal using Delphi Program', *jtm*, vol. 12, no. 2, pp. 102–108, Jun. 2011, doi: 10.9744/jtm.12.2.102-108.